Average circuit model for angle-controlled STATCOM

M. Tavakoli Bina and D.C. Hamill

Abstract: A static compensator (STATCOM) is a FACTS controller, whose capacitive or inductive output current can be controlled independently of the AC system voltage. A practical ± 75 kVAr STATCOM has been designed, in which the phase difference between the converter voltage and the AC system voltage is controlled over a small region to obtain a nearly linear reactive power control. The converter voltage is synthesised using a PWM control with a fixed modulation index close to one. Here it is modelled using an averaging approach, by deriving the state–space equation of the STATCOM in the time domain. An average operator is defined, and applied to the state equation to get an averaged mathematical model. Expansion of this model will eventually lead to an average circuit model. An approximate averaged switching function represents the duty ratio as a continuous function of time. The solution is expandable as a Fourier series, which can be suitably truncated. Theoretical considerations show that the averaged model should agree well with the original system, and this is confirmed by MATLAB and PSpice simulations. Experimental results provide some practical waveforms that, compared to the corresponding simulations, validate the developed models.

1 Introduction

The use of FACTS (flexible AC transmission systems) controllers can potentially overcome disadvantages of electromechanically controlled transmission systems. The static compensator (STATCOM), as a parallel device in AC power systems, is analysed in [1–3]. The analysis of a power electronics system is complex, due to its switching behaviour. Therefore there is a need for simpler, approximate models. One common approach to the modelling of power converters is averaging. This approximates the operation of the discontinuous system by a continuous-time model. As well as simplifying analysis and making it easier to understand the system's behaviour under steady-state and transient conditions, averaged models have the advantage that they speed up simulation.

To develop an average model for STATCOM, this paper first starts with its time-varying state–space equations. They are approximated by averaged equations, giving a mathematical model. Then an equivalent circuit model is introduced, which provides a useful tool for analytical purposes. The average model gives good agreement with the original system, as demonstrated using MATLAB and PSpice simulations as well as practical work. Note that a STATCOM is different from a perfect supply (an ideal three-phase generator, neglecting both the leakage inductance and the moment of inertia of the rotor masses), because the converter voltage is dependent on its DC-side voltage, and the DC voltage varies as a function of the relative phase angle of the converter voltage. Thus, three-phase ideal sources are unable to model not only the consequences of DC-voltage dynamic behaviour but also the switching waveforms, giving different results from those of the average and exact models. The average models consider this vital dynamic behaviour of the DC-side capacitor as well as the switch-mode converter, and approximates the exact system by neglecting high-frequency details on STATCOM waveforms.

2 STATCOM operating principles

Figure 1a shows a three-phase STATCOM. Let the angle α be defined as the phase separation between the fundamental components of v and v'. When α is zero, by varying v', reactive power can be controlled. To provide the required active and reactive powers by STATCOM, α varies in a small nonzero region around zero (the bigger this region the lower the performance of the converter due to nonlinearity issues) [1]. In fact, changing α will also vary the DC voltage V_C, and consequently v'. In [1–3], the explained mode of operation is modelled by transforming the system to a synchronous frame, showing a stable system with oscillatory dynamic response for STATCOM. A typical steady-state operation of STATCOM as a function of α is shown in Fig. 1b. Three state variables i_d, i_q, and V_C give the equivalent active current, reactive current and DC voltage, respectively, showing nearly linear functions of α. This suggests a way of controlling STATCOM, mainly by α.

2.1 Practical issues

A ± 75 kVAr angle-controlled STATCOM was developed for a distribution substation. Here 21 600 samples per cycle are taken from the low-voltage side (400 V) of the substation and stored in an EPROM. Thus, the spacing between successive pulses is one minute, the accuracy of the controlled angle α is 0.5′ (minute) or half a sample pulse

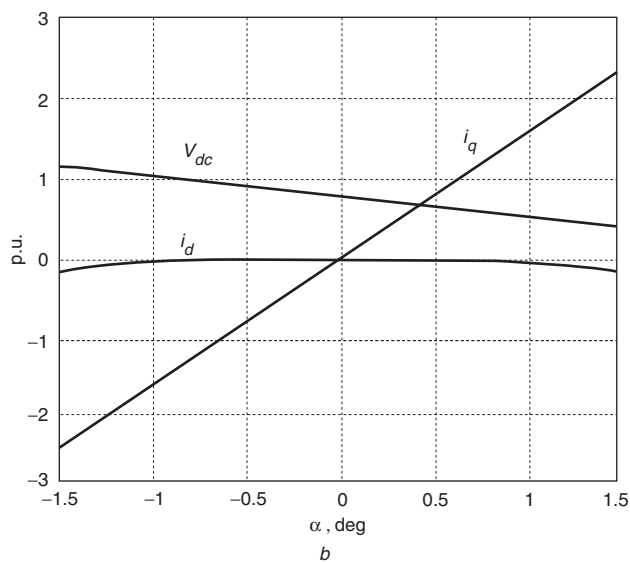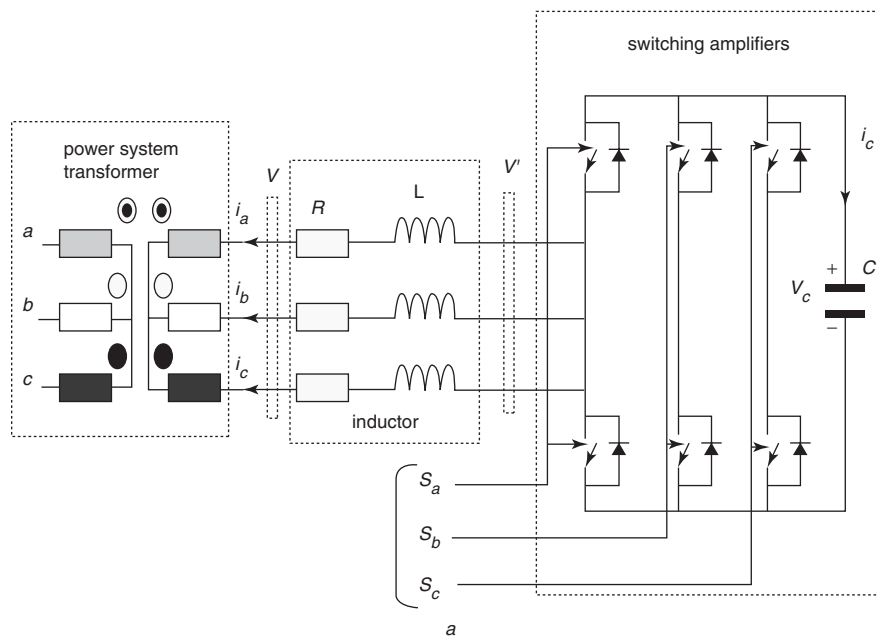*IEE Proc.-Electr. Power Appl., Vol. 152, No. 3, May 2005*

653

Fig. 1

a Three-phase circuit of STATCOM

b Reactive and active currents (normalised by the STATCOM nominal current), and DC voltage (normalised by the uncontrolled full-bridge rectifying DC voltage) as functions of α

width in the worst case. The device operates at mains frequency of 50 Hz, with an operating control range of $\alpha \in [-1.5°, 1.5°]$, which fulfils the ratings of the designed device. Hence, to control reactive power flow to 1% of rated power (here 0.75 kVAr), an accuracy of 0.9′ (minute) is required (equivalent to 0.83 μs in the time domain or 0.0021 Hz in the frequency domain), which can be achieved by the employed device.

Using the electronic circuit, the frequency of the mains supply is determined with a phase-locked loop (PLL), and multiplied by 21 600 within the PLL. This resultant frequency is then used as a clock for a counter showing the address of the reference EPROM. At the same time, any change in the relative phase angle α is added instantly to this address, and the counter reset to the resulting address. Simultaneously, a parallel circuit integrates the changes in the relative phase angle and stores an instantaneous α as the initial value. Whenever a zero voltage detector (ZVD) detects the zero-crossing of the mains supply voltage, the counter is reset to this initial value to manage a fast and

accurate phase correction. Therefore, the IGBT-based converter and modern control electronics give the STAT-COM a dynamic performance capability far exceeding that of other reactive power compensators. Another EPROM stores the triangular carrier with the same clock as the reference EPROM. Thus, the PWM modulator always operates at an exact multiple of the mains supply frequency. Here $M = 45$ (480 samples per triangular waveform) was chosen for the device, which is an odd multiple of three.

3 Averaging principles

State–space averaging (SSA) was established by Middle-brook and Cuk [4]. Then, a review in [5] surveyed the Bogoliubov theorem for finding a bound for approximation of the time-varying state equation by averaging. The averaging theory discussed in [5, 6] has been extended to cases in which state discontinuities occur [7].

654

IEE Proc.-Electr. Power Appl., Vol. 152, No. 3, May 2005

3.1 Application to STATCOM

Assume that the converter voltage is synthesised using a PWM control, and the control loop focuses on α over a linear region to get the required operational setting points (see Fig. 1b). There are two main periods involved in STATCOM: the reference period T_R (obtained from the mains supply frequency) and the switching period T_C (depending on T_R), the period of the PWM carrier. The open-loop average equations are obtained in a standard form that can later be modified for closed-loop control:

$$x(t) = f(x(t), s(t), u(t)) \qquad (1)$$

where $x(t)$ is the state vector $[i_a(t), i_b(t), V_C(t)]^T$, $u(t)$ is the input vector and $s(t) = [s_a(t), s_b(t), s_c(t)]^T$ is the vector of switching function. This latter consists of a sequence of M pulses ($M = T_R/T_C$, an odd multiple of three). Note that at this stage the duty ratio is *not* considered to be a continuous function of time, but rather a discrete value associated with an individual switching period. Now the averaging operator

$$\xi_a(t) = \text{average } \xi(t) \triangleq \frac{1}{T_C} \int_{t-T_C}^{t} \xi(\tau)d\tau \qquad (2)$$

is applied to (1) over $[t\text{-}T_C, t]$, to get an average model described by

$$\dot{x}_a(t) = g(x_a(t), D(t), u(t)) \qquad (3)$$

where $x_a(t)$ is the average state vector, and $D(t)$ is the approximate continuous duty ratio that is controlled by α and affected by switching period T_C. Starting from (1) and (3), a theorem in [7] describes the closeness of $x(t)$ and $x_a(t)$. Assuming $x(0) = x_a(0)$, for any small $\delta > 0$ and large $N > t_0$ (take $t_0 = 0$ here), there exists a T_0 (a function of δ and N) and a positive constant K such that for switching period $T_C \in [0, T_0]$, provided $x(0) = x_a(0)$, then $\|x(t) - x_a(t)\| \le \delta e^{KN}$. In fact, $x(t)$ and $x_a(t)$ can remain close to each other, provided the switching period is small enough. Another theorem in [8] states that, if $x_a(t)$ approaches an asymptotically stable equilibrium point, then there exists a sufficiently small T_0 (a function of δ) such that for switching period $T_C \in [0, T_0]$, $\|x(t) - x_a(t)\| \le \delta$. Therefore, if the averaged model is asymptotically stable, which is generally true, $x(t)$ will be very close to $x_a(t)$. This validates the averaging approach to modelling STATCOM.

3.2 Periodic coefficient differential equations

The state space model of (1) includes a discrete switching function along with the mains supply applied voltage. A switching pulse will *not* necessarily repeat itself exactly after time T_C. The switching period T_C contains two time intervals t_{on} (the upper switch is closed) and t_{off} (the upper switch is opened). These two time intervals differ for the pulses within the supply period T_R. Thus, the period of the switching function is T_R rather than T_C, although the number of switching transitions during T_C is fixed. Hence, for a periodic PWM reference, M different pulses of width T_C are repeated every cycle of the mains supply. Therefore, M different sets of coefficients provide a periodic description of STATCOM in state-space form. The bigger the multiplier M, the more complicated the exact model of STATCOM. Hence, this complex power electronics system needs to be described by a simpler, approximate model. Note that the average model leads eventually to a single set of differential equations stated by (3) along with an approximate duty ratio.

4 Average model of STATCOM

The foregoing methodology is now applied to develop a state–space average model of STATCOM. Consider the STATCOM shown in Fig. 1a. There are two topological modes for every leg. The state equations for the two modes can be obtained separately and then, introducing the switching function $s(t) \in \{-1, 1\}$, combined into a single state equation:

$$\dot{x}(t) = (A_r + A_a s_a(t) + A_b s_b(t) + A_c s_c(t))x(t) + bu(t)$$

$$A_r = \begin{bmatrix} -\dfrac{R}{L} & 0 & 0 \\ 0 & -\dfrac{R}{L} & 0 \\ 0 & 0 & 0 \end{bmatrix}, \quad A_a = \begin{bmatrix} 0 & 0 & \dfrac{1}{3L} \\ 0 & 0 & \dfrac{-1}{6L} \\ \dfrac{-1}{2C} & 0 & 0 \end{bmatrix},$$

$$A_b = \begin{bmatrix} 0 & 0 & \dfrac{-1}{6L} \\ 0 & 0 & \dfrac{1}{3L} \\ 0 & \dfrac{-1}{2C} & 0 \end{bmatrix}, \quad A_c = \begin{bmatrix} 0 & 0 & \dfrac{-1}{6L} \\ 0 & 0 & \dfrac{-1}{6L} \\ \dfrac{1}{2C} & \dfrac{1}{2C} & 0 \end{bmatrix}$$

$$x(t) = \begin{bmatrix} i_a(t) & i_b(t) & V_C(t) \end{bmatrix}^T,$$

$$b = \begin{bmatrix} \dfrac{-2}{3L} & \dfrac{1}{3L} & \dfrac{1}{3L} \\ \dfrac{1}{3L} & \dfrac{-2}{3L} & \dfrac{1}{3L} \\ 0 & 0 & 0 \end{bmatrix}, \quad u(t) = \begin{bmatrix} v_a(t) \\ v_b(t) \\ v_c(t) \end{bmatrix} \qquad (4)$$

Then (4) is averaged over a switching period to develop a time-continuous model, in the form of (3). Applying the averaging operator of (2), let $x_a(t)$, the averaged state vector, be defined as

$$x_a(t) = \frac{1}{T_C} \int_{t-T_C}^{t} x(\tau)d\tau \qquad (5)$$

It can also be shown that

$$\dot{x}_a(t) = \frac{1}{T_C} \int_{t-T_C}^{t} \frac{dx(\tau)}{d\tau}d\tau \qquad (6)$$

Integrating (4) over $[t-T_C, t]$ and applying (5), we get

$$\begin{aligned} \dot{x}_a(t) = & A_r \frac{1}{T_C} \int_{t-T_C}^{t} x(\tau)d\tau + A_a \frac{1}{T_C} \\ & \int_{t-T_C}^{t} s_a(\tau)x(\tau)d\tau + A_b \frac{1}{T_C} \\ & \int_{t-T_C}^{t} s_b(\tau)x(\tau)d\tau + A_c \frac{1}{T_C} \\ & \int_{t-T_C}^{t} s_c(\tau)x(\tau)d\tau + b \frac{1}{T_C} \int_{t-T_C}^{t} u(\tau)d\tau \end{aligned} \qquad (7)$$

The waveform of $s(\tau)$ during $[t-T_C, t]$ has four possible forms, as shown in Fig. 2. Each of these forms can be substituted as the switching waveform in the right-hand side of (7), Taking the worst case leads us to
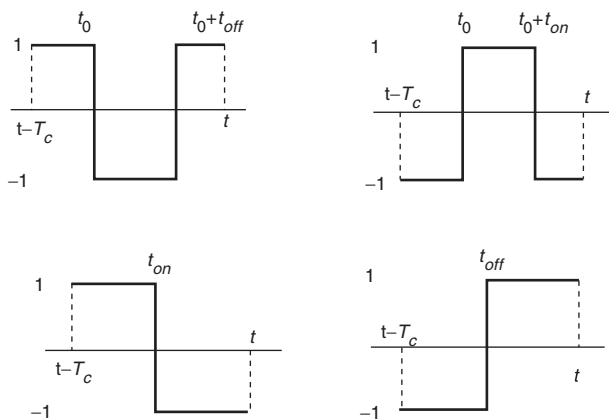
Fig. 2 *Four possible forms of s(t) over [t-T_C, t]*

$$\frac{1}{T_C}\int_{t-T_C}^{t} s(\tau)x(\tau)d\tau = (2D_i(t)-1) \tag{8}$$
$$x_a(t) + e(t) \quad i = a, b, c$$

Here $D(t) = t_{on}(t)/T_C$, where $t_{on}(t)$ is the sub-interval of $[t-T_C, t]$, during which the upper switch is closed. The Appendix provides an extended error analysis, introducing an upper bound for the error term $e(t) \leq \frac{\dot{x}(t)T_C}{2}$. If the average of $x(\tau)$ taken over T_C is close to its average taken over the sub-interval, the error term in (8), $\dot{x}(t)T_C/2$, will be negligible. The slower the variation of $x(t)$ and the higher the PWM carrier frequency, the smaller the error. This clearly relates the switching frequency to the performed analysis as well as the power system perturbation frequency. Integrating the PWM switching functions in Fig. 2 over $[t-T_C, t]$, the switching function average is

$$\int_{t-T_C}^{t} s(\tau)d\tau = 2D_i(t) - 1 \quad i = a, b, c \tag{9}$$

defining the continuous duty-ratio function $D(t)$. The resultant averaged state equation is

$$\begin{aligned}\dot{x}_a(t) = &(A_r + A_a(2D_a(t) - 1) \\ &+ A_b(2D_b(t) - 1) \\ &+ A_c(2D_c(t) - 1)x_a(t) + b\bar{u}(t)\end{aligned} \tag{10}$$

where $\bar{u}(t)$ is the average of the input $u(t)$. These two vectors are approximately the same because the mains supply waveforms vary slowly compared to the averaging period. In practice, $D(t)$ has a sinusoidal waveform. Here therefore the special case is considered where the PWM has a ramp carrier waveform and a sinusoidal reference of $m\sin(\omega t - \pi/2)$, m being the modulation index. From the Fourier series for $s_a(t)$, its fundamental phasor $S_1 = me^{-j\pi/2}$ is substituted in (9) and (10) (the DC term and higher harmonics being

neglected), to find the continuous $D_a(t)$ as

$$D_a(t) \approx$$
$$\begin{cases} \frac{1}{2}\left[1 + m\frac{\sin(\pi/M)}{\pi/M}\sin\left(\omega t - \frac{\pi}{M} + \alpha\right)\right] \\ 0 \leq m \leq 1 \\ \begin{cases} 1 & \sin^{-1}\left(\frac{1}{m}\right) \leq \omega t - \frac{\pi}{M} + \alpha \leq \pi - \sin^{-1}\left(\frac{1}{m}\right) \\ 0 & \pi + \sin^{-1}\left(\frac{1}{m}\right) \leq \omega t - \frac{\pi}{M} + \alpha \leq 2\pi - \sin^{-1}\left(\frac{1}{m}\right) \quad m > 1 \\ \frac{1}{2}\left[1 + m\frac{\sin(\pi/M)}{\pi/M}\sin\left(\omega t - \frac{\pi}{M} + \alpha\right)\right] & \text{otherwise} \end{cases} \end{cases} \tag{11}$$

Similar approximations could be given for $D_b(t)$ and $D_c(t)$. Note that the phase angle π/M will not be different for three phases when M is chosen as an odd multiple of three.

A MATLAB program was written to calculate the error between the exact duty ratio (at $t = nT_C$, $n = 1, 2,\ldots,M$) and the continuous approximation in (11). For $M = 45$, the worst-case error is less than 1.5%.

4.1 Closed-loop control
The principle of closed-loop STATCOM control is presented in [1], assuming the states of the power system are available for feedback. Figure 3 shows the control scheme, where the power system consists of a number of generators, transformers and transmission lines along with several STATCOMs connected across selected busbars. The PI control in Fig. 3 includes two gains K_i (integral part) and K_p (proportional part) to control the voltage response of the STATCOM. The angles α_{min} and α_{max} are the relative phase angle limits, which are imposed by the maximum reactive power capability as well as the DC voltage of STATCOM. Consider that the system is linearised about an operating
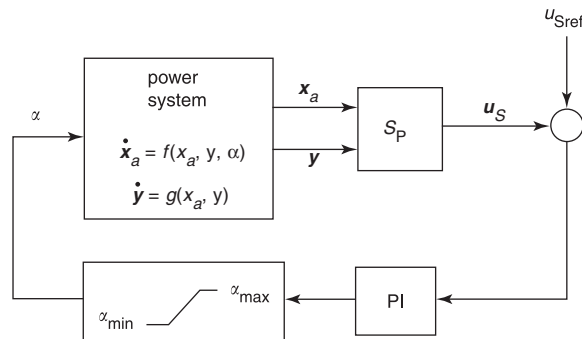

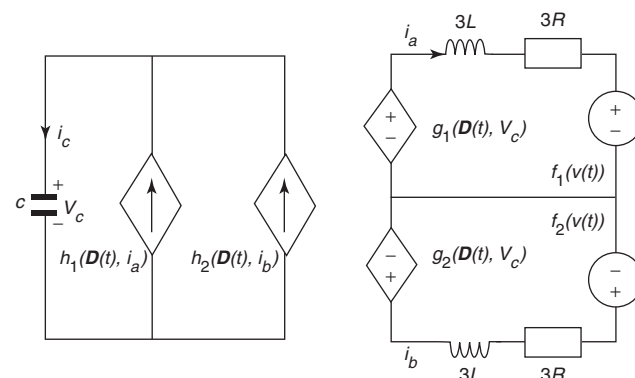**Fig. 3** *Control of voltage response of STATCOM using a PI control scheme*

Fig. 4 *Equivalent circuit average model of STATCOM, suitable for circuit simulators such as SPICE*

point, and the generator model is given by

$$\dot{y} = Cy + Du \tag{12}$$

Using (10), the STATCOM model can be rewritten as

$$\dot{x}_a = A(t)x_a + bu \tag{13}$$

where $A(t)$ is a periodic matrix, and the states x_a and y are coupled through an algebraic network equation (u and $\bar{u}$ are almost the same, see above):

$$Ex_a + Fy + Gu = 0 \tag{14}$$

Now, if G is invertible, then the feedback control gain K_{FB} can be expressed by ([1])

$$K_{FB} = K_i Q_P - K_P S_P G^{-1} E \tag{15}$$

where S_P and Q_P are the matrices of the position of STATCOMs and the PI controllers within the power system, respectively.

5 Average circuit model

To get the average circuit model, first two independent voltage sources

$$[f_1(u(t)) \quad f_2(u(t))]^T = \\ [2v_a(t) - v_b(t) - v_c(t) \quad 2v_b(t) - v_a(t) - v_c(t)]^T \tag{16}$$

along with two voltage-controlled voltage sources (VCVS) are defined as follows:

$$[g_1(D(t)) \quad g_2(D(t))]^T = \\ [V_C(2D_a(t) - D_b(t) - D_c(t)) \\ V_C(2D_b(t) - D_a(t) - D_c(t))]^T \tag{17}$$

Three state equations (10) describe the average inductor currents and capacitor voltage.

The first two equations can be interpreted as meaning that the average inductor currents depend on the voltage difference between the independent sources (16) and dependent sources (17). The third equation shows that the average current of capacitor C is composed of two current-controlled current sources (CCCS) h_1 and h_2, each as a function of duty ratios and line currents, namely,

$$[h_1(D(t), i_a(t)) \quad h_2(D(t), i_b(t))]^T = \\ [i_a(t)(D_c(t) - D_a(t)) \quad i_b(t)(D_c(t) - D_b(t))]^T \tag{18}$$

The resulting equivalent circuit model is shown in Fig. 4, and is suitable for circuit simulators such as SPICE. Note that the capacitor circuit should be connected to the inductor circuits using two very big impedances Z for PSpice simulation purposes, which leaves negligible effect on the circuit behaviour.

6 Simulation results

This Section compares various simulation results for STATCOM and the provided models, performed with MATLAB and PSpice. The parameters used here are based on those of a practical STATCOM designed for a distribution substation. Hence, the provided experimental waveforms in comparison with the performed simulations validate the proposed models. It should be noted that a distinct 100 Hz oscillation on the exact DC voltage is not present in the average model, but it will be reproduced by improving the model in future study.

6.1 MATLAB simulation

First, the average model of STATCOM was simulated. The input voltage was $u(t) = 155.6[\sin(\omega t + \pi/2) \quad \sin(\omega t +$
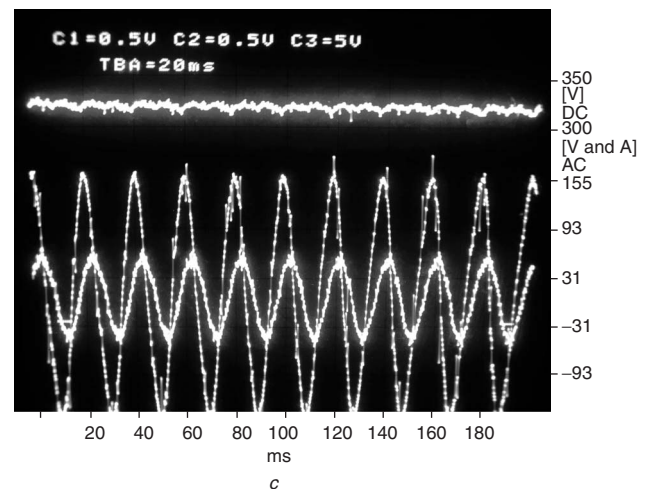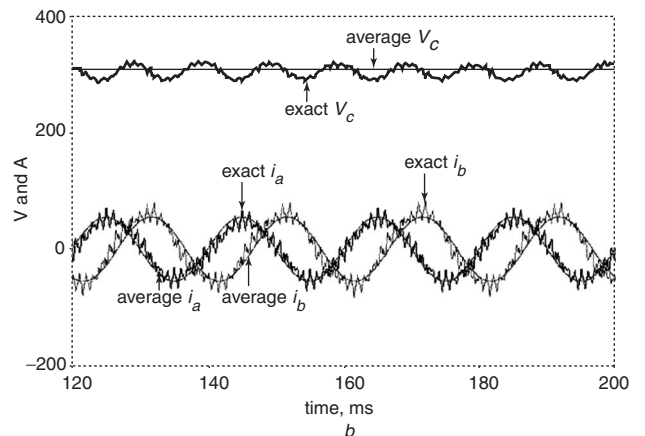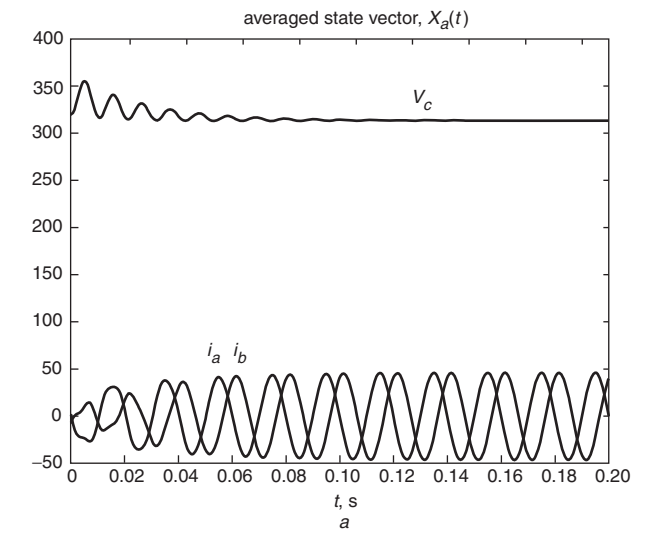

Fig. 5 *Simulation results for average model of STATCOM, operating in inductive mode ($\alpha = 1°$)*
a MATLAB simulating average mathematical model
b PSpice simulating average circuit model
c Experimental results validating both simulations and models

$\pi/2 - 2\pi/3) \quad \sin(\omega t + \pi/2 - 2\pi/3)]^T$, with $L = 1.0\,\text{mH}$, $C = 1.2\,\text{mF}$ and $R = 0.06\,\Omega$ The initial state vectors were $x(0) = x_a(0) = [0, \quad -10,320]^T$ and modulation index was fixed to 0.9. Figures 5a and 6a show the state variables of STATCOM for two cases: $\alpha = 1°$ (inductive mode) and $\alpha = -1°$ (capacitive mode).

These results show that the capacitor voltage tends to increase for $\alpha = -1°$ while it decreases for $\alpha = 1°$; both

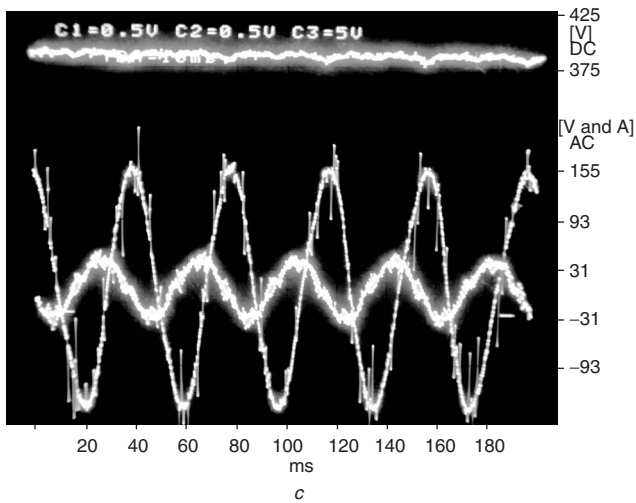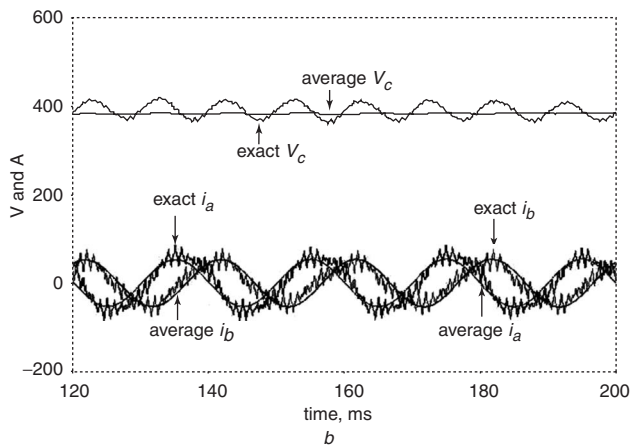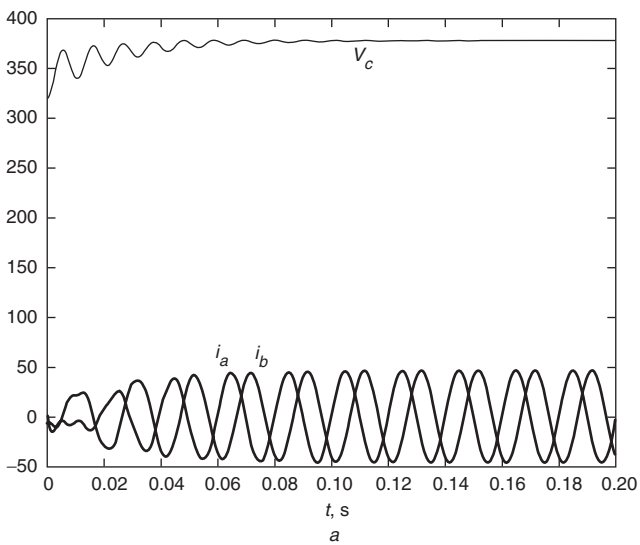**Fig. 6** *Simulation results for average model of STATCOM, operating in capacitive mode $(\alpha = -1°)$*
a MATLAB simulating average mathematical model
b PSpice simulating average circuit model
c Experimental results validating both simulations and models

converge to certain steady-state conditions. These are also illustrated by Fig. 1*b*. The line currents i_a and i_b can be added together to get the other line current i_c.

6.2 PSpice simulation results
The equivalent circuit model of Fig. 4 together with the exact switched-system model of Fig. 1 were simulated with

PSpice. The parameters are the same as for the MATLAB simulations of Figs. 5 and 6. Figures 5*b* and 6*b* show the state variables for both exact and average models. Apart from the ripples, the agreement is good, demonstrating the compatibility of the average model for the involved perturbation frequency. The PSpice simulation results can also be compared with those of MATLAB, presented in Fig. 5. Again the agreement is good, validating the equivalent circuit as well as the mathematical average model. But the average model ran much faster than the exact model, offering useful savings in situations where accurate waveforms are not important (e.g. investigating system transients).

6.3 Experimental results
Figures 5*c* and 6*c* provide a typical STATCOM current along with the capacitor voltage for both inductive and capacitive modes. Agreement is good between the presented simulations and the practical outcomes, validating the introduced models.

6.4 Application example
As an application of the developed circuit model, a transient of STATCOM was simulated with PSpice. Initially, STATCOM is injecting reactive power $(\alpha = -1°)$. At $t = 130$ ms, the relative phase angle is changed to $\alpha = 1°$ using a step function, which forces the STATCOM to absorb the same reactive power. Figure 7*a* shows this simulation, containing both the exact and average
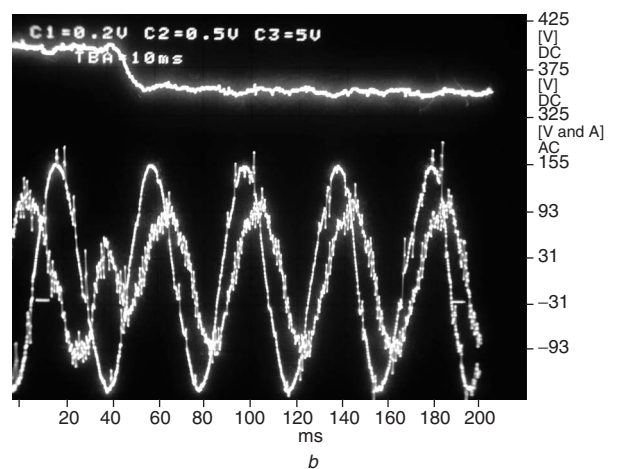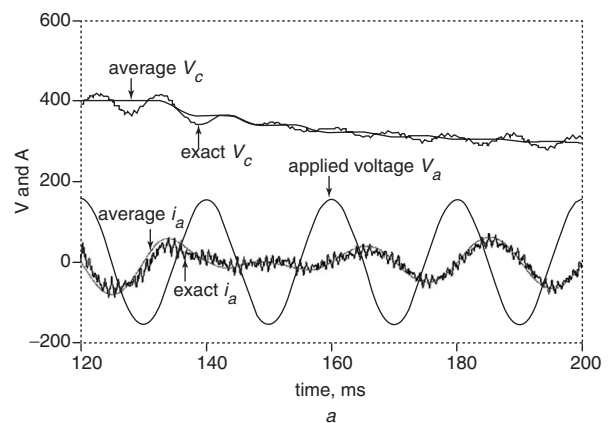

Fig. 7 *Transient of STATCOM, changing from capacitive mode $(\alpha = -1°)$ to inductive mode $(\alpha = -1°)$ using step function*
a PSpice simulating both exact and average circuit models
b Experimental results validating simulations

waveforms of capacitor voltage V_C and the inductor current i_a. Also, the applied voltage v_a is included. Similarly, Fig. 7b shows experimental results for the transient case, which again validate the average model simulations. Both the simulation and the practical work take about one cycle to approach their new operating point.

7 Conclusions

A theoretically sound averaging method has been applied to approximate the behaviour of STATCOM. Starting with the exact state equations, an average model was developed. An equivalent circuit model was derived from the resulting equations. The exact system (simulated with PSpice and obtained by practical work) and the approximate model (simulated with MATLAB and PSpice) are all in good agreement, verifying that the necessary and sufficient conditions of the averaging theorems in [7] are satisfied by the proposed models.

8 References

1 Rao, P., Crow, M.L., and Yang, Z.: 'STATCOM control for power system voltage control application', *Applied Power Electronics Conf.*, 2000, **15**, (4), pp. 1311–1317
2 Gyugyi, L.: 'Dynamic compensation of AC transmission lines by solid-state synchronous voltage source', *IEEE Trans. Power Deliv.*, 1994, **9**, (2), pp. 904–911
3 Gyugyi, L., Hingorani, N.G., and Nannery, P.R.: 'Advanced static VAr compensator using gate turn-off thyristors for utility application'. CIGRE Conf. Rec., 1990 Session, pp. 23–27
4 Middlebrook, R.D., and Cuk, S.: 'A general unified approach to modeling switching-converter power stages'. Proc. Power Electronics Specialists Conf., 1976, pp. 18–34
5 Lehman, B., and Bass, R.M.: 'Switching frequency dependent averaged models for PWM DC-DC converters', *IEEE Trans. Power Electron.*, 1996, **11**, (1)
6 Krein, P.T., Bentsman, J., Bass, R.M., and Lesieutre, B.L.: 'On the use of averaging for the analysis of power electronic systems', *IEEE Trans. Power Electron.*, 1990, **5**, (2), pp. 182–190
7 Lehman, B., and Bass, R.M.: 'Extension of averaging theory for power electronic systems', *IEEE Trans. Power Electronics*, 1996, **11**, (4)
8 Lehman, B., Bentsman, J., Lunel, S.V., and Verriest, E.: 'Vibrational control of nonlinear time lag systems: averaging theory, stabilizability, and transient behaviour', *IEEE Trans. Autom. Control*, 1994, **39**, (5), pp. 898–912

9 Appendix

Error Analysis

Here the details of the error analysis are presented. First, the error term in (8) is introduced for the four possible cases illustrated in Fig. 2. Second, an upper bound is assigned to the error term. Let $e(t)$ be the error term. Consider the waveform in the top left part of Fig. 2. By substituting its parameters in the second term of (8), we have

$$
\frac{1}{T_C}\int_{t-T_C}^{t} s(\tau)x(\tau)d\tau =
$$
$$
\frac{1}{T_C}\left[\int_{t-T_C}^{t_0} x(\tau)d\tau - \int_{t_0}^{t_0+t_{off}} x(\tau)d\tau + \int_{t_0+t_{off}}^{t} x(\tau)d\tau\right] \tag{19}
$$

Assuming $t_0 = t - T_C + \gamma$, and $\beta = t - t_0 - t_{off}$ in this waveform, we have $\gamma + \beta = t_{on} = D(t)T_C$. Considering another assumption $\int_a^b x(t)dt = y(b) - y(a)$, (19) could be rewritten as:

$$
\frac{1}{T_C}\int_{t-T_C}^{t} s(\tau)x(\tau)d\tau
$$
$$
= \frac{1}{T_C}\{y(t) - y(t-T_C)
$$
$$
- 2y(t-\beta) + 2y(t-T_C+\gamma)\} \tag{20}
$$

Now, $y(t-T_C)$, $y(t-\beta)$, and $y(t-T_C+\gamma)$ are expanded by their Taylor series (γ, β, and T_C being very small). For example, $y(t - T_C) = y(t) - T_C\dot{y}(t) + \frac{T_C^2}{2}\ddot{y}(t)$ where the higher terms are ignored as T_C is very small, and $y(t)$ is smooth. Substituting these relationships in (20), leads us to:

$$
\frac{1}{T_C}\int_{t-T_C}^{t} s(\tau)x(\tau)d\tau
$$
$$
= \frac{1}{T_C}\{\dot{y}(t)(2D(t)-1)
$$
$$
+ \ddot{y}(t)\left(\frac{-T_C}{2} - (1-D(t))(\gamma-\beta-T_C)\right)\} \tag{21}
$$

The first term on the right-hand side is the average $(\dot{y}(t)(2D(t)-1) = x_a(t)(2D(t)-1))$, and the second term is the error $e(t)$. A similar procedure was carried out for the other three waveforms in Fig. 2. The resulting error functions are:

$$
e(t) = \begin{cases} \dot{x}_a(t)\left(\frac{-T_C}{2} - (1-D(t))(\gamma-\beta-T_C)\right) \\ \dot{x}_a(t)\left(\frac{T_C}{2} - D(t)(-\gamma+\beta+T_C)\right) \\ \dot{x}_a(t)T_C(D(t)^2 - 2D(t) + 1/2) \\ \dot{x}_a(t)T_C(D(t)^2 - 1/2) \end{cases} \tag{22}
$$

Now an upper bound is assigned to the error function. The error function has four different forms, as given in (22). Here it is shown that the error function always obeys $e(t) \leq \dot{x}_a(t)\frac{T_C}{2}$. Considering the top left waveform in Fig. 2; it is clear that $\frac{|\beta-\gamma|}{T_C} < \frac{t_{on}}{T_C} = D(t)$. As $1 + \frac{\beta-\gamma}{T_C} \leq 1 + \left|\frac{\beta-\gamma}{T_C}\right| \leq 1 + D(t)$, it can easily be found that $e(t) \leq \dot{x}_a(t)T_C(-D(t)^2 + 1/2)$. $D(t)$ varies over [0,1], resulting in $-1/2 \leq -D(t)^2 + 1/2 \leq 1/2$. This implies that $e(t) \leq \dot{x}_a(t)\frac{T_C}{2}$. This was also carried out for the other three waveforms, resulting in the same upper bound for all possible cases in the worst case. As a result of this analysis, $e(t)$ in (8) is substituted by $\dot{x}(t)\frac{T_C}{2}$.

IEE Proc.-Electr. Power Appl., Vol. 152, No. 3, May 2005

659